Yamaoka *et al. Earth, Planets and Space* (2016) 68:175
DOI 10.1186/s40623-016-0548-4

Earth, Planets and Space

PREFACE

Open Access

# Special issue "The phreatic eruption of Mt. Ontake volcano in 2014"

Koshun Yamaoka[1*], Nobuo Geshi[2], Takeshi Hashimoto[3], S. E. Ingebritsen[4] and Teruki Oikawa[2]

## Introduction

Mt. Ontake volcano erupted at 11:52 on September 27, 2014, claiming the lives of at least 58 hikers. This eruption was the worst volcanic disaster in Japan since the 1926 phreatic eruption of Mt. Tokachidake claimed 144 lives (Table 1). The timing of the eruption contributed greatly to the heavy death toll: near midday, when many hikers were near the summit, and during a weekend of clear weather conditions following several rainy weekends. The importance of this timing is reflected by the fact that a somewhat larger eruption of Mt. Ontake in 1979 resulted in injuries but no deaths. In 2014, immediate precursors were detected with seismometers and tiltmeters about 10 min before the eruption, but the eruption started before a warning was issued.

The Coordinating Committee for Prediction of Volcanic Eruption met the next day to investigate observations by institutions such as the Japan Meteorological Agency (JMA). They concluded that the eruption was phreatic, based on analysis of volcanic ash collected immediately after the eruption, and also concluded that the eruption could evolve to a magmatic one, based on experience at other volcanoes. Urgent research began under the Grants-in-Aid for Scientific Research program funded by the Japan Society for the Promotion of Science (JSPS). This special issue was planned to collect the research carried out in response to the 2014 eruption of Mt. Ontake.

Before reviewing the papers in this issue, we summarize the recent activity of Mt. Ontake and selected results from JMA monitoring. Magmatic activity is relatively low in comparison with other active volcanoes in Japan. Geological studies show that at least four magmatic eruptions occurred over the past 10,000 years, the most recent from Gonoike crater around 6000 years ago, and that phreatic eruptions occurred every several hundred years (Oikawa et al. 2015). No historical records of eruptions prior to 1979 have been found, although fumarolic activity in the Jigukudani valley to the southwest of the summit (Fig. 1) has been reported for the past several hundred years (Oikawa 2008).

On October 28, 1979, the first recorded eruption in human history occurred, a phreatic eruption with total discharged mass of about 200,000 tons corresponding to VEI 2. This eruption opened new craters near the top of Jigukudani valley (Fig. 1). In 1991, a very small phreatic eruption occurred from one of the vents created by the 1979 eruption. In 2007, another small eruption occurred from the same vent, and a very long period (VLP) earthquake and crustal deformation were detected (Nakamichi et al. 2009). No further eruptions occurred until September 2014.

Figure 2 shows results of long-term monitoring by the JMA. Fumarole height data (Fig. 2a) are lacking from 1981 to 1988 but show a relatively low level of activity during 3-year periods before both the 2007 and 2014 eruptions. Fumarole vent temperatures, measured intermittently, decayed through 2012, although there are few more recent measurements (Fig. 2b). Seismic activity near the summit has been monitored from 1988 to present and increased in association with the eruptions in 1991 and 2007 (Fig. 2c). The level of seismic activity was low during the 3-year period before September 2014.

JMA detected unusual seismic activity on September 10–11, 2014, two weeks before the eruption. Daily events counts were the largest since the 2007 eruption, but no volcanic tremor or crustal deformation was detected. Low-frequency earthquakes were detected, but were much fewer in number than those observed in association with the 2007 eruption. This is the main reason that the JMA chose not to raise the volcano warning level, and makes comparison between the 2007 and 2014 eruptions a primary issue in many of these studies.

*Correspondence: kyamaoka@seis.nagoya-u.ac.jp
[1] Graduate School of Environmental Studies, Nagoya University, Nagoya, Japan
Full list of author information is available at the end of the article

**Table 1 List of recent Japanese eruptions that claimed >10 lives (supplemented to Japan Meteorological Agency 2013)**

| Date (Y/M/D) | Volcano | Victims | Description |
|---|---|---|---|
| 1721/6/22 | Asama | 15 | Ballistic ejecta |
| 1741/8/18 | Oshima-Oshima | 1467 | Tsunami |
| 1779/11/8-9 | Sakurajima | >150 | Ballistic ejecta and lava flow |
| 1781/4/11 | Sakurajima | 15 | Tsunami caused by an off-shore eruption |
| 1783/8/5 | Asama | 1151 | Pyroclastic flow, mud flow and flood by a collapse of natural dam |
| 1785/4/18 | Aogashima | 130–140 | Phreatomagmatic eruption? |
| 1792/5/21 | Unzen | >15,000 | Debris avalanche and tsunami caused by it |
| 1822/3/12 | Usu | 50 | Pyroclastic flow |
| 1856/9/25 | Hokkaido-Koma | 21–29 | Ballistic ejecta and pumice flow |
| 1888/7/15 | Bandai | 461 | Debris avalanche |
| 1900/7/17 | Adatara | 73 | Destruction of a sulfur mine |
| 1902/8/7 | Izu-Torishima | 125 | Phreatomagmatic eruption |
| 1914/1/12 | Sakurajima | 58–59 | Ballistic ejecta and lava flow |
| 1926/5/24 | Tokachidake | 144 | Mud flow |
| 1940/7/12 | Miyake | 11 | Ballistic ejecta |
| 1952/9/24 | Bayonnaise | 31 | Phreatomagmatic explosion with submarine eruption |
| 1958/6/24 | Aso | 31 | Ballistic ejecta |
| 1991/6/3 | Unzen | 43 | Pyroclastic flow |
| 2014/9/27 | Ontake | 58 (+5 missing) | Ballistic ejecta |

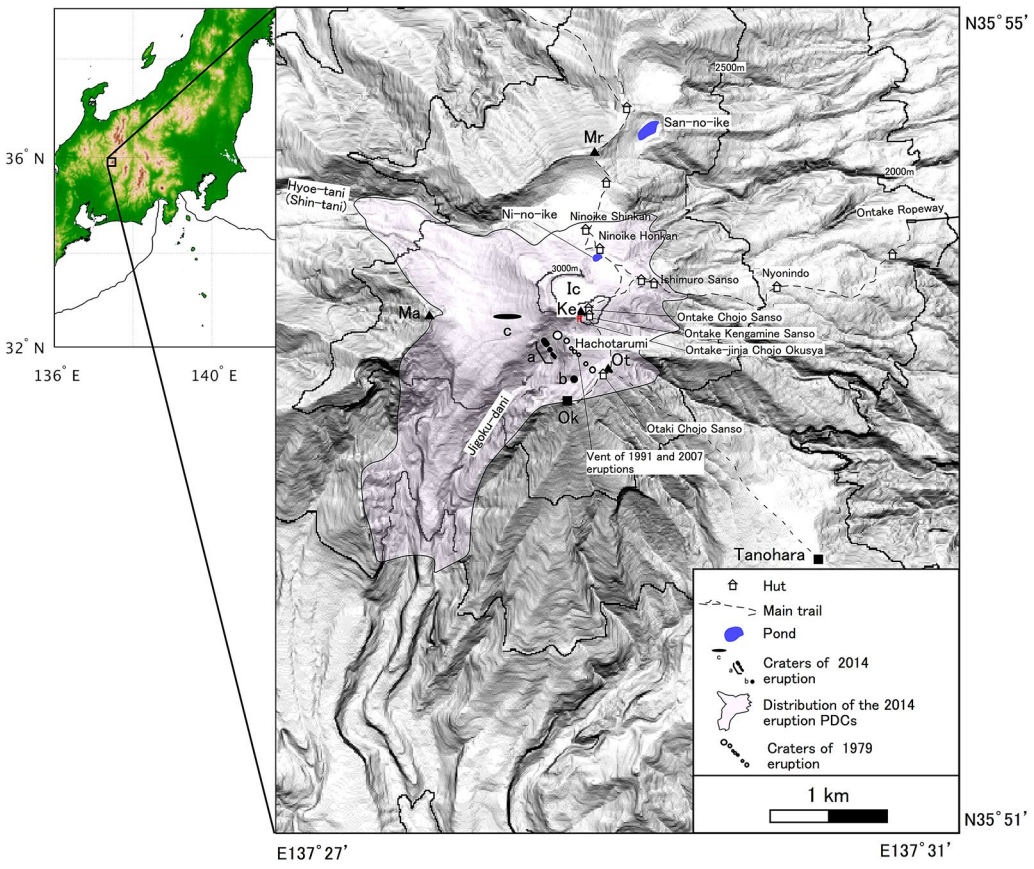


**Fig. 1** Location map of Mt. Ontake volcano, modified from Fig. 1 of Oikawa et al. (2016)

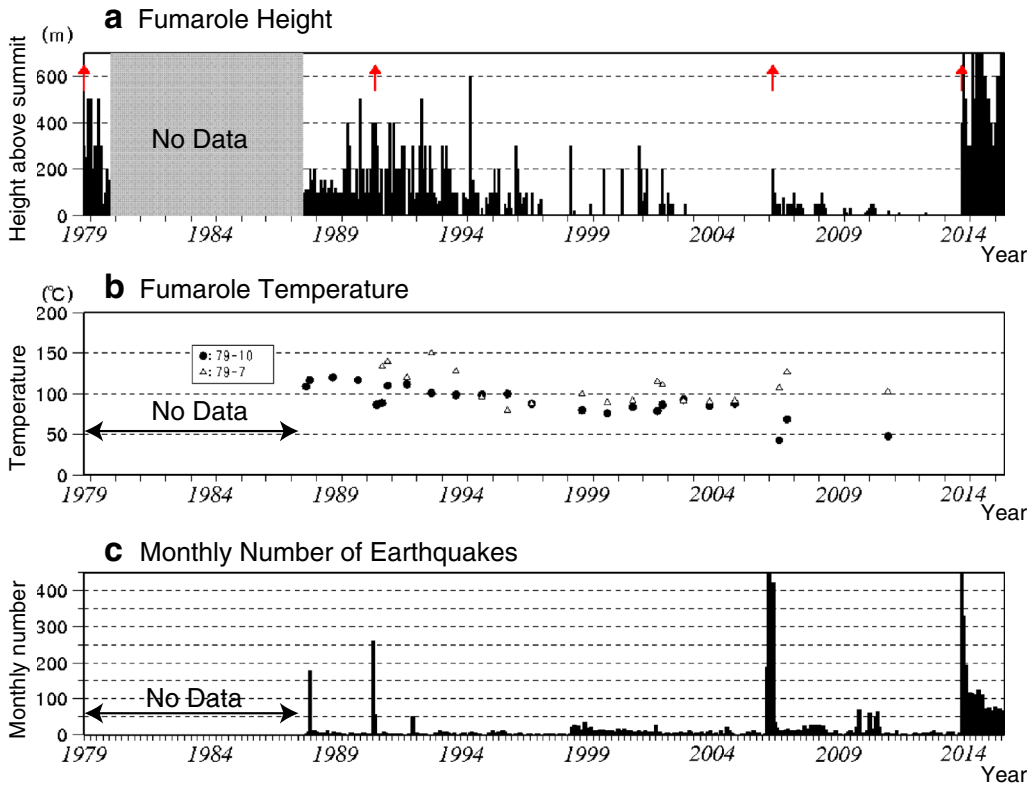


**Fig. 2** Results of long-term monitoring of volcanic activity by the Japan Meteorological Agency: **a** fumarole height based on visual measurements; **b** fumarole temperature measured at an active vent of the 1979 eruption; **c** monthly number of earthquakes near the summit of Mt. Ontake. Earthquakes are counted for the same station under a constant criterion using S-P time and maximum amplitude in seismograms

## Contents of the special issue

In this section, we briefly review the papers of the special issue together with related papers published in other journals. The papers are classified into five categories depending on the principal study methodology.

### Visual observations

The 2014 eruption of Mt. Ontake provided an unusually rich set of visual records of phreatic eruption. Hikers near the crater took still photographs and videos from many locations immediately after the onset of the eruption. Researchers took photographs and videos from news-media helicopters in good weather conditions. These visual data are valuable for process studies of phreatic eruptions, which have rarely if ever been recorded in such detail. Two papers (Kaneko et al. 2016; Oikawa et al. 2016) are based mainly on the visual data; see also Maeno et al. (2016) for eruption chronology based on combined analysis of visual images and the tephra sequence.

Kaneko et al. (2016) describe the spatial characteristics of the eruption based in large part on aerial observations made the following day. Three major craters opened at the head of Jigukudani valley (Fig. 1); the central crater was the main vent. A pyroclastic density current (PDC) with relatively low destructive force travelled approximately 2.5 km downvalley from this central vent. Ballistics ejecta emerged tens of seconds after the beginning of the eruption, reached distances of up to 950 m from the vent, and attained maximum initial velocities estimated at 111 m/s.

Oikawa et al. (2016) describe the sequence of the eruption based on interviews and visual records such as still photographs and videos taken by hikers, which provide precise time records of the eruption. The interviewees included mountain guides and workers in mountain huts. Oikawa et al. (2016) divide the eruption into three phases: PDC flow, pyroclastic fall with muddy rain, and muddy water overflowing from the crater. The eruption began with dry pyroclastic density currents and without any precursory surface phenomena. The temperature of the PDCs in the summit area was generally 30–100 °C. During the period over which the PDCs covered the surface, many lapilli and volcanic block-sized ballistic ejecta fell within 1 km of the crater.

### Geological observations

During the 2014 Mt. Ontake eruption tephra was ejected as PDC, ballistics, and air fall. Takarada et al. (2016)

and Maeno et al. (2016) document the total volume of tephra and the size of the eruption and Sasaki et al. (2016) describe the resulting lahar. Kaneko et al. (2016) and Tsunematsu et al. (2016) analyze the distribution of ballistic ejecta and Tsunematsu et al. (2016) simulate ballistic trajectory and calculate a landing energy of $10^4$ J, essential data for future shelter designs.

Takarada et al. (2016) estimate discharged mass of the fallout deposit by a segment-integration method and find a total mass of around $1 \times 10^6$ tons, more than 90% of which occurs proximal to the craters. The discharged mass of the 2014 eruption is about half that of the 1979 eruption.

Sasaki et al. (2016) describe the syneruptive-spouted type lahar generated by water directly emitted from the craters. The lahar flowed downvalley south of the crater to a distance of 5 km. A rough estimate of the emplaced volume is $1.2 \times 10^5$ m$^3$, about 1/10 of the total discharge volume. The chemical characteristics of the lahar material are the same as those of the tephra, indicating a common origin.

Maeno et al. (2016) reconstruct the eruption sequence based on observations of PDC and fallout deposits in the proximal area near the crater. The deposits indicate that the eruption began dry but evolved to wet. The deposits show, from bottom to the top, gravity-driven dilute PDCs from the vent-opening phase; fallout from a vigorous moist plume during vent development; and wet ash fall. The particle concentration and initial flow velocity of the PDCs are estimated to be $2 \times 10^{-4}$–$2 \times 10^{-3}$ and 24–56 m/s, respectively.

Tsunematsu et al. (2016) estimate ejection velocities of ballistic projectiles by comparing simulation results with the observations by Kaneko et al. (2016). To account for the observed distribution in the summit area, ballistic projectiles are ejected at a vertical angle of 20° from vertical and at an azimuthal angle 20° clockwise from the north. The optimal ejection velocity is 145–185 m/s for a particle diameter of 20 cm with a drag coefficient of 0.62–1.01, and the mean landing energy is of the order of $10^4$ J.

### Seismological observations

Seismological observations are used to analyze source processes of earthquakes and tremors and locate their sources. Kato et al. (2015) and Zhang and Wen (2015) provide detailed descriptions of the hypocenters associated with the eruption. Maeda et al. (2015) infer crack opening immediately before the eruption. Ogiso et al. (2015) track the source location of tremor beneath the crater. Finally, Terakawa et al. (2016) reveal stress changes associated with the eruption, strongly implying fluid-pressure changes.

Kato et al. (2015) perform a high-resolution analysis of seismicity associated with the 2014 eruption using a matched-filter detection technique. They succeed in relocating the volcano-tectonic earthquakes (VT) and long-period earthquakes (LP) from August and September 2014. VT seismic activity increased from 6 September to 11 September, and a change in the frequency-magnitude distribution of the seismic activity (b-value) was also observed. During the 10-minute period before the eruption, VT earthquakes migrated upward and extended in a N–S direction, which roughly coincides with the orientation of the newly opened vents. The authors emphasize that hypocenter migration immediately before the eruption may reflect the movement of hydrothermal fluids to the surface.

Zhang and Wen (2015) (*Geophysical Research Letters*) apply the match-and-locate method to detect and precisely locate seismic activity associated with the 2007 and 2014 eruptions. The results for 2007 show less variation in the epicenter location than those associated with the 2014 eruption, consistent with the results of Kato et al. (2015).

Maeda et al. (2015) analyze a very long period earthquake (VLP event) that occurred 25 s before the start of the eruption and infer opening of an ENE-WSW-oriented tensile crack at a depth of 0.3–1 km from the surface. They infer that hydrothermal fluid flowed through the crack toward the surface.

Ogiso et al. (2015) use the spatial amplitude distribution of tremor data associated with the eruption to track the source location of the tremor. They find that it was located beneath the crater and descended 2 km over the course of several minutes following the onset of the eruption; this appears to be a robust solution.

Terakawa et al. (2016) (*Nature Communications*) analyze temporal change in the focal mechanism of earthquakes beneath the craters to document the stress variation associated with the phreatic eruption. Substantial deviation from the average stress field is observed in the focal mechanism in the period before the phreatic eruption.

### Geodetic observations

Geodetic observation reveals deformation processes and can permit direct estimation of the location and geometry of the source of deformation. The four papers dealing with geodetic observations all consider both the 2007 and 2014 eruptions.

Takagi and Onizawa (2016) use Global Navigation Satellite System (GNSS) observations and model the inflation that occurred before the 2007 eruption as a volume increase of $6 \times 10^6$ m$^3$, mainly as crack opening (diking) at an estimated depth of 5 km below sea level. A smaller volume change of $0.38 \times 10^6$ m$^3$ at a depth of about 1 km beneath the surface is estimated for the period before

the 2014 eruption. The apparent lack of deeper volume change prior to the 2014 eruption is viewed as consistent with the water-level observations of Koizumi et al. (2016).

Koizumi et al. (2016) analyze a groundwater-pressure monitoring record maintained from 1998 on at a borehole 10 km southeast of the summit. That record shows a clear drop in pressure prior to the 2007 eruption but no pressure change before or after the 2014 eruption, consistent with the inference of little or no additional magmatic intrusion.

Miyaoka and Takagi (2016) apply a stacking method to increase the signal-to-noise ratio of GNSS data and compare the period before the 2014 eruption to that before the 2007 eruption. The 2014 data reveal minor crustal deformation caused by volume change in a shallow source beginning one month before the eruption. The volume change is unresolvable but appears similar to that associated with the 2007 eruption.

Murase et al. (2016) use leveling-survey and GNSS data from 2002-present to estimate a source model of crustal deformation. Data from 2006 to 2007 are used to construct a model of crack opening for the 2007 eruption. From 2007 to 2013, no GNSS change was observed, but leveling surveys showed uplift on the eastern flank, suggesting continued crack opening there. During the 2014 eruption, baseline shortening and subsidence was observed, indicating deflation of the source beneath the summit.

#### Observations and analysis of the hydrothermal system

Geochemical study of volcanic fluids and tephra provides detailed information regarding the hydrothermal system that appears to have fed the eruption. Five papers show the possible range of depth and temperature of the source region as well as process that may connect the hydrothermal system with underlying magma. Based on the lack of juvenile materials, sulfur isotope equilibrium temperatures of 270–280 °C, and some indications of magmatic influence, these eruptions may be classified as "hydrothermal eruptions," in which most of eruption energy is derived from the hydrothermal system itself, indirectly influenced by deeper magmatic intrusion.

Ikehata and Maruoka (2016) analyze pyroclastic material from the 2014 eruption and show that it derives from acidic alteration zones. Sulfur isotope systematics show that the pyroclastic material equilibrated at a temperature of 270–280 °C. Pyroclastic material from the somewhat larger 1979 eruption is very similar in terms of mineral assemblage and sulfur isotope composition, with the exception of the sulfur isotope composition of anhydrite.

Minami et al. (2016) compare the mineral assemblage of the volcanic ash from the 2014 eruption with the well-known mineralogy of porphyry copper systems. The ash contains partly altered volcanic rock fragments and volcanic glass accompanied by alteration minerals, as is typical of non-juvenile hydrothermal-eruption deposits. The mineral composition indicates that the ash was derived from depths of less than 2 km.

Mori et al. (2016) describe a series of measurements of volcanic gas near the 2014 eruption vents which reveal that the volcanic gas was not directly emitted from magma but was influenced by hydrothermal system. The $SO_2$ flux was more than 2000 t/day one day after the onset of the eruption but decreased to 130 t/day over the course of the following two months. Taking the significant decline in the $SO_2/H_2S$ ratio into account, it is likely that the $H_2S$ flux remained about 700–800 t/day for two months after the onset of the eruption. Such a sustained high flux of $H_2S$ is a peculiar feature of Mt. Ontake relative to other major volcanoes. A similar pattern of variation was observed following the 1979 eruption.

Sano et al. (2015) (*Nature Communications*) describe the results of intermittent monitoring (13 samples/33 years) of helium-isotope data from 1981 to present in the vicinity of Mt. Ontake. These data show an increasing $^3He/^4He$ ratio from 2000 to 2014 at the site nearest to the crater. This suggests increasing contribution of mantle helium and may reflect magmatic activity beneath Mt. Ontake volcano.

Sabry and Mogi (2016) mapped the electrical resistivity structure beneath Mt. Ontake using a GREATEM (GRounded Electrical source Airborne Transient ElectroMagnetic) system. A low-resistivity layer beneath the eastern flank of the volcano suggests the presence of a hydrothermal zone at around 500 m depth, potentially connected to the phreatic eruption.

## Discussion

#### Shallow source structure

Several lines of evidence indicate that the source of the phreatic eruption was very shallow, originating beneath the crater at depths of less than 2 km and possibly less than 1 km. Geochemical study of volcanic fluids and tephra implies that the erupted materials came from a shallow hydrothermal system below the summit. This inference is consistent with analysis of the single VLP event (suggesting opening at 0.3–1 km depth) and models for geodetic deformation. The earthquake hypocenter locations (Kato et al. 2015) are 1–2 km deeper than the depth of the source of the phreatic eruption estimated from other methods. This inconsistency may result from uncertainty regarding the shallow seismic-velocity structure. Improved seismic-velocity mapping of Mt. Ontake would allow better hypocenter location beneath the summit area.

Since the 2014 eruption, the crater area has deflated at a nearly constant rate (Fig. 3). InSAR analysis (Narita and Murakami 2016) shows that ongoing deflation at a rate of 2–3 $\times$ $10^5$ $m^3$ per year is also shallow-rooted (0.5 km depth) and localized, consistent with continued depressurization of the hydrothermal system. Post-eruption heat-discharge rates and the corresponding water mass fluxes are larger (order $10^4$–$10^5$ tons per day, Terada 2014) than the deflation volume estimated with geodetic observations, suggesting continued contribution of additional hydrothermal fluids from larger, deeper source areas. A low-resistivity structure mapped by Sabry and Mogi (2016) extends beneath both the crater and eastern flank and suggests a possible connection to a larger hydrothermal system. The leveling survey by Murase et al. (2016) documents uplift and subsidence on the eastern flank between 2007 and 2014, possibly related to a hydrothermal system beneath the eastern flank.

### Suggestions for future disaster mitigation

Most of the precursors that we rely on to forecast volcanic eruptions depend upon detection of fluid movement or its consequences. Because of the shallow source region and the low viscosity of the moving fluids, phreatic eruptions such as the 2014 eruption of Mt. Ontake can occur with little warning; fluid movement may begin only minutes in advance of eruption. However, obvious and potentially useful seismic and geodetic precursors may be detected tens of seconds to tens of minutes before eruption. In the case of the 2014 eruption of Mt. Ontake, rapid growth of tremor activity (Fig. 3 of Ogiso et al. 2015) and tilting (Fig. 7 of Takagi and Onizawa 2016) were observed about 7 min before the eruption. From the standpoint of public safety, it is therefore useful to consider options for communicating very short-term warning of phreatic eruptions. Given the short time frame, warnings may need to be generated automatically by means of an objective algorithm and communicated directly to the public by devices such as sirens or cellular devices.

Longer-term "precursors" such as changes in ground level (Murase et al. 2016) and helium-isotope ratios (Sano et al. 2015) have also been documented at Mt. Ontake. However, given the long-term (annual to decadal) evolution of these phenomena, and the inherent intermittency of the data, these observations are not useful for near-real-time forecasting. They can be very useful for retrospective process understanding.

There were also midterm (days) changes in seismic activity prior to the 2014 eruption of Mt. Ontake. The implications of the midterm seismic changes were regarded as ambiguous in real time. No complementary geodetic deformation was observed, but retrospective analysis of geodetic data (Miyaoka and Takagi 2016) confirmed that minor near-summit deformation did occur. An improved local geodetic network or analysis of InSAR data might have facilitated near-real-time interpretation of midterm seismic and geodetic changes.

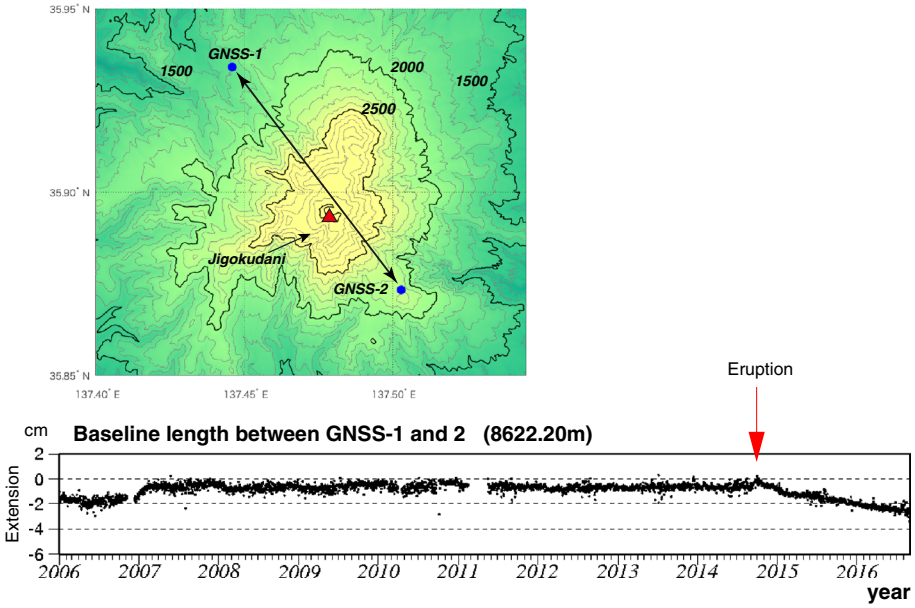


**Fig. 3** Temporal change in baseline length between GNSS-1 (Ochiai-Karatani station) and GNSS-2 (Tanohara station); GNSS plot courtesy of the Japan Meteorological Agency

It is possible that magmatic intrusion prior to 1979 initiated the recent sequence of phreatic eruptions (1979, 1991, 2007, 2014) by adding heat and magmatic volatiles to the hydrothermal system. This speculation is consistent with increasing $^{3}He/^{4}He$ ratios observed since 1981 in proximal samples (Sano et al. 2015). The nature of geodetic deformation in 2007 suggests additional intrusion of new magma at mid-crustal depths of approximately 5 km. Although none of the recent eruptions have ejected juvenile material, the possibility of magma eruption remains, and the officials concerned with forecasting and public safety must consider the possibility that purely phreatic eruptions will evolve into phreatomagmatic eruptions.

It also seems possible, perhaps likely, that the recent cycle of phreatic eruptions at Mt. Ontake (1979, 1991, 2007, 2014) reflects repeated pressurization and breaching of the shallow hydrothermal system. In the absence of seismicity and associated fracturing, there is a fairly universal tendency for permeability to decrease due to mineral precipitation and other hydrothermal-alteration processes (Gleeson and Ingebritsen 2016). Thus, diminished fumarolic activity may reflect a period of sealing and pressurization of the shallow hydrothermal system; fractures begin to open or shear when fluid pressure is sufficiently elevated.

Monitoring and forecasting capability might be improved by deploying additional geophysical- and geochemical-monitoring capabilities in the near vicinity of the summit crater. Magnetometers will be deployed to monitor the magnetic total field, which may help to map ongoing hydrothermal alteration and temperature changes at relatively shallow depths. Gas monitoring will also help to understand the ongoing hydrothermal processes. Generating continuous long-term time series will require sustained effort in a remote near-summit environment that is characterized by extreme weather and discharge of high-temperature, low-pH hydrothermal fluids.

The 2014 eruption provides some lessons regarding public safety in the context of phreatic eruption. Most fatalities were related to impact ejecta. At Mt. Ontake, there was a window of several tens of seconds before the first ballistic impacts (Kaneko et al. 2016), which achieved energy on the order of $10^4$ J (Tsunematsu et al. 2016). Thus, the public should be aware of nearby structures or natural features that can provide shelter from ejecta. The temperature of the PDC in this specific case was 30–100 °C (Oikawa et al. 2016), but could potentially have been higher because the temperature at the hydrothermal source is estimated to have been 270–280 °C (Ikehata and Maruoka 2016). Whereas the fatalities caused by ballistic impact occurred within 1 km of the vent, the vent-sourced lahar traveled about 5 km, sufficient distance to threaten nearby communities and affect the pH and turbidity of water supplies (Sasaki et al. 2016); thus, there is also potential for more distal damage.

**Author details**
[1] Graduate School of Environmental Studies, Nagoya University, Nagoya, Japan. [2] Geological Survey of Japan, Advanced Industrial, Science and Technology, Tsukuba, Japan. [3] Faculty of Science, Hokkaido University, Sapporo, Japan. [4] United States Geological Survey, Menlo Park, CA, USA.

Received: 12 October 2016 Accepted: 14 October 2016
Published online: 10 November 2016

**References**

Gleeson T, Ingebritsen SE (eds) (2016) Crustal permeability. AGU/Wiley Blackwell, Chichester

Ikehata K, Maruoka T (2016) Sulfur isotopic characteristics of volcanic products from the September 2014 Mount Ontake eruption, Japan. Earth Planets Space 68:116. doi:10.1186/s40623-016-0496-z

Japan Meteorological Agency (2013) National catalogue of the active volcanoes in Japan, 4th edn. Japan Meteorological Agency, Chiyoda

Kaneko T, Maeno F, Nakada S (2016) 2014 Mount Ontake eruption: characteristics of the phreatic eruption as inferred from aerial observations. Earth Planets Space 68:72. doi:10.1186/s40623-016-0452-y

Kato A, Terakawa T, Yamanaka Y, Maeda Y, Horikawa S, Matsuhiro K, Okuda T (2015) Preparatory and precursory processes leading up to the 2014 phreatic eruption of Mount Ontake, Japan. Earth Planets Space 67:111. doi:10.1186/s40623-015-0288-x

Koizumi N, Sato T, Kitagawa Y, Ochi T (2016) Groundwater pressure changes and crustal deformation before and after the 2007 and 2014 eruptions of Mt. Ontake. Earth Planets Space 68:48. doi:10.1186/s40623-016-0420-6

Maeda Y, Kato A, Terakawa T, Yamanaka Y, Horikawa S, Matsuhiro K, Okuda T (2015) Source mechanism of a VLP event immediately before the 2014 eruption of Mt. Ontake, Japan. Earth Planets Space 67:187. doi:10.1186/s40623-015-0358-0

Maeno F, Nakada S, Oikawa T, Yoshimoto M, Komori J, Ishizuka Y, Takeshita Y, Shimato T, Kaneko T, Nagai M (2016) Reconstruction of a phreatic eruption on 27 September 2014 at Ontake volcano, central Japan, based on proximal pyroclastic density current and fallout deposits. Earth Planets Space 68:82. doi:10.1186/s40623-016-0449-6

Minami Y, Imura T, Hayashi S, Ohba T (2016) Mineralogical study on volcanic ash of the eruption on September 27, 2014 at Ontake volcano, central Japan: correlation with porphyry copper systems. Earth Planets Space 68:67. doi:10.1186/s40623-016-0440-2

Miyaoka K, Takagi A (2016) Detection of crustal deformation prior to the 2014 Mt. Ontake eruption by the stacking method. Earth Planets Space 68:60. doi:10.1186/s40623-016-0439-8

Mori T, Hashimoto T, Terada A, Yoshimoto M, Kazahaya R, Shinohara H, Tanaka R (2016) Volcanic plume measurements using a UAV for the 2014 Mt. Ontake eruption. Earth Planets Space 68:49. doi:10.1186/s40623-016-0418-0

Murase M, Kimata F, Yamanaka Y, Horikawa S, Matsuhiro K, Matsushima T, Mori H, Ohkura T, Yoshikawa S, Miyajima R, Inoue H, Mishima T, Sonoda T, Uchida K, Yamamoto K, Nakamichi H (2016) Preparatory process preceding the 2014 eruption of Mount Ontake volcano, Japan: insights from precise leveling measurements. Earth Planets Space 68:9. doi:10.1186/s40623-016-0386-4

Nakamichi H, Kumagai H, Nakano M, Okubo M, Kimata F, Ito Y, Obara K (2009) Source mechanism of a very-long-period event at Mt Ontake, central Japan: response of a hydrothermal system to magma intrusion beneath the summit. J Volcanol Geotherm Res 187:167–177

Narita S, Murakami M (2016) Deflation source after the September 2014 eruption of Ontake Volcano, Japan detected by ALOS2/PALSAR2 InSAR. Abstract, Japan Geoscience Union Meeting 2016, SVC47-26

Ogiso M, Matsubyashi H, Yamamoto T (2015) Descent of tremor source locations before the 2014 phreatic eruption of Ontake volcano, Japan. Earth Planets Space 67:206. doi:10.1186/s40623-015-0376-y

Oikawa T (2008) Reinvestigation of the historical eruption and fumarolic activity records at Ontake Volcano, central Japan. Bull Geol Surv Japan 59(5–6):203–210

Oikawa T, Suzuki Y, Chiba T, Kishimoto H, Okuno M, Ishizuka O (2015) Holocene eruption hisotry of the Ontake Volcano, central Japan. Abstracts, Fall Meeting of the Volcanological Society of Japan, 102 **(in Japanese)**

Oikawa T, Yoshimoto M, Nakada S, Maeno F, Komori J, Shimano T, Takeshita Y, Ishizuka Y, Ishimine Y (2016) Reconstruction of the 2014 eruption sequence of Ontake Volcano from recorded images and interviews. Earth Planets Space 68:79. doi:10.1186/s40623-016-0458-5

Sabry AA, Mogi T (2016) Three-dimensional resistivity modeling of GREATEM survey data from Ontake Volcano, northwest Japan. Earth Planets Space 68:76. doi:10.1186/s40623-016-0433-z

Sano Y, Kagoshima T, Takahata N, Nishio Y, Roullearu E, Pinti DL, Fischer P (2015) Ten-year helium anomaly prior to the 2014 Mt Ontake eruption. Sci Rep 5:13069. doi:10.1038/srep13069

Sasaki H, Chiba T, Kishimoto H, Naruke S (2016) Characteristics of the syneruptive-spouted type lahar generated by the September 2014 eruption of Mount Ontake, Japan. Earth Planets Space 68:141. doi:10.1186/s40623-016-0516-z

Takagi A, Onizawa S (2016) Shallow pressure sources associated with the 2007 and 2014 phreatic eruptions of Mt. Ontake, Japan. Earth Planets Space 68:135. doi:10.1186/s40623-016-0515-0

Takarada A, Oikawa T, Furukawa R, Hoshizumi H, Itoh J, Geshi N, Miyagi I (2016) Estimation of total discharged mass from the phreatic eruption of Ontake Volcano, central Japan, on September 27, 2014. Earth Planets Space 68:138. doi:10.1186/s40623-016-0511-4

Terada A (2014) Heat-discharge activities from the Jigokudani crater at Ontake volcano after the phreatic eruption in September 2014. Abstract, Fall meeting of Volcanological Society of Japan, UP-24 **(in Japanese)**

Terakawa T, Kato A, Yamanaka Y, Maeda Y, Horikawa S, Matsuhiro K, Okuda T (2016) Monitoring eruption activity using temporal stress changes at Mount Ontake volcano. Nat Commun 7:10797. doi:10.1038/ncomms10797

Tsunematsu K, Ishimine Y, Kaneko T, Yoshimoto M, Fujii T, Yamaoka K (2016) Estimation of ballistic block landing energy during 2014 Mount Ontake eruption. Earth Planets Space 68:88. doi:10.1186/s40623-016-0463-8

Zhang M, Wen L (2015) Earthquake characteristics before eruptions of Japan's Ontake volcano in 2007 and 2014. Geophys Res Lett 42:6982–6988. doi:10.1002/2015GL065165